Biomimetic Synthesis of Inorganic Nanospheres

Jeng-Shiung Jan, Seungju Lee, C. Shane Carr, and Daniel F. Shantz*

Department of Chemical Engineering, Texas A&M University, College Station Texas 77843

Received February 25, 2005. Revised Manuscript Received June 13, 2005

The synthesis of silica, silver bromide, and composite nanospheres made in the presence of block copolypeptide vesicles is reported. Hollow silica nanospheres of controllable size can be made with Lys:Phe 1:1 block copolypeptides, whereas at higher block ratios, uniform silica nanospheres are formed that are not hollow. Silver bromide nanospheres of controllable size in the range of 25−250 nm can also be formed, as well as silver bromide/silica core−shell particles. The silver bromide nanospheres can also be assembled into hollow rods in the presence of rhodamine 6G, and this process is reversible. The unique feature of this work is the ability to translate the information of an individual biomimetic supramolecular structure (e.g., vesicle) as a template into an inorganic material. The results show that block copolypeptides offer unique opportunities for assembling nanostructured materials.

Introduction

Developing new approaches to fabricating metals, metal oxides, and other hard matter wherein structure can be well controlled at the nanometer length scale is a research field of tremendous interest.[1] To achieve the goal of controlling nanoscale structure, numerous approaches are currently being explored including microemulsion-mediated synthesis of nanoparticles,[2,3] templating of nanostructured materials using self-assembled polymer/surfactant microstructures,[4−6] material formation/growth in confined spaces,[7−10] hydrothermal/solvothermal treatment,[11−13] and chemical vapor deposition[14] to name just a few. Taking this a step further, the ability to control structure independently on multiple length scales simultaneously will open up new possibilities for nanostructured materials in a range of fields including catalysis, separations, sensing, and micro- or nanoelectronics. Finally, for simplicity of processing, a synthetic methodology that utilizes self-assembly would clearly be desirable. Given the enormous interest in controlling structure and function over multiple length scales, this is an area that will undoubtedly continue to be actively pursued.

While chemists, physicists, materials scientists, and engineers have made significant headway in this area, nature is already an expert. Consider that nature has (1) developed the ability to synthesize macromolecules (proteins) comprised of simple monomer units (amino acids) that have unparalleled structural features on multiple length scales because of primary, secondary, tertiary, and quaternary structure[15,16] and (2) developed the ability to fabricate inorganic and inorganic−hybrid materials such as silica diatoms and nacre that have properties that the materials science community can only aspire to achieve.[17−30] Materials such as bone, nacre, and silica diatoms are supreme examples of the complex yet highly controllable hierarchically structured materials nature

* Author to whom correspondence should be addressed. Phone: (979) 845−3492; fax: (979) 845−6446; e-mail: Shantz@che.tamu.edu.

(1) Law, M.; Goldberger, J.; Yang, P. *Annu. Rev. Mater. Res.* **2004**, *34*, 83−122.
(2) Pileni, M. P. *Catal. Today* **2000**, *58*, 151−166.
(3) Pileni, M. P. *Langmuir* **1997**, *13*, 3266−3276.
(4) Imhof, A.; Pine, D. J. *Nature* **1997**, *389*, 948−951.
(5) Kresge, C. T.; Leonowicz, M. E.; Roth, W. J.; Vartuli, J. C.; Beck, J. S. *Nature* **1992**, *359*, 710−712.
(6) Zhao, D.; Feng, J.; Huo, Q.; Melosh, N.; Fredrickson, G. H.; Chmelka, B. F.; Stucky, G. D. *Science* **1998**, *279*, 548−552.
(7) Wu, Y.; Cheng, G.; Katsov, K.; Sides, S. W.; Wang, J.; Tang, J.; Fredrickson, G. H.; Moskovits, M.; Stucky, G. D. *Nat. Mater.* **2004**, *3*, 816−822.
(8) Yamaguchi, A.; Uejo, F.; Yoda, T.; Uchida, T.; Tanamura, Y.; Yamashita, T.; Teramae, N. *Nat. Mater.* **2004**, *3*, 337−341.
(9) Lu, Q. Y.; Gao, F.; Komarneni, S.; Mallouk, T. E. *J. Am. Chem. Soc.* **2004**, *126*, 8650−8651.
(10) Wang, D. H.; Kou, R.; Yang, Z. L.; He, J. B.; Yang, Z. Z.; Lu, Y. F. *Chem. Commun.* **2005**, 166−167.
(11) Lu, Q.; Gao, F.; Komarneni, S. *J. Am. Chem. Soc.* **2004**, *126*, 54−55.
(12) Li, Y.; Wang, J.; Deng, Z.; Wu, Y.; Sun, X.; Yu, D.; Yang, P. *J. Am. Chem. Soc.* **2001**, *123*, 9004−9005.
(13) Manna, L.; Milliron, D. J.; Meisel, A.; Scher, E. C.; Alivisatos, A. P. *Nat. Mater.* **2003**, *2*, 382−385.
(14) Wu, Y.; Xiang, J.; Yang, C.; Lu, W.; Lieber, C. M. *Nature* **2004**, *430*, 61−65.
(15) Creighton, T. E. *Proteins: Structures and Molecular Principles*; W. H. Freeman: New York, 1993.
(16) Branden, C.; Tooze, J. *Introduction to Protein Structure*; Garland: New York, 1999.
(17) Baeuerlein, E. *Biomineralization: From Biology to Biotechnology and Medical Application*; Wiley-VCH: Weinheim, Germany, 2000.
(18) Soellner, C.; Burghammer, M.; Busch-Nentwich, E.; Berger, J.; Schwarz, H.; Reikel, C.; Nicolson, T. *Science* **2003**, *302*, 282−286.
(19) Zhou, Y.; Shimizu, K.; Cha, J. N.; Stucky, G. D.; Morse, D. E. *Angew. Chem., Int. Ed.* **1999**, *38*, 780−782.
(20) Poulsen, N.; Sumper, M.; Kroeger, N. *Proc. Natl. Acad. Sci. U.S.A.* **2003**, *100*, 12075−12080.
(21) Kroeger, N.; Deutzmann, R.; Sumper, M. *Science* **1999**, *286*, 1129−1132.
(22) Kroeger, N.; Deutzmann, R.; Bergsdorf, C.; Sumper, M. *Proc. Natl. Acad. Sci. U.S.A.* **2000**, *97*, 14133−14138.
(23) Kroeger, N.; Lorenz, S.; Brunner, E.; Sumper, M. *Science* **2002**, *298*, 584−586.
(24) Naik, R. R.; Whitlock, P. W.; Rodriguez, F.; Brott, L. L.; Glawe, D. D.; Clarson, S. J.; Stone, M. O. *Chem. Commun.* **2003**, 238−239.
(25) Reches, M.; Gazit, E. *Science* **2003**, *300*, 625−627.
(26) Sumper, M. *Science* **2002**, *295*, 2430−2433.
(27) van Bommel, K. J. C.; Friggeri, A.; Shinkai, S. *Angew. Chem., Int. Ed.* **2003**, *42*, 980−999.
(28) Wong, M. S.; Cha, J. N.; Choi, K. S.; Deming, T. J.; Stucky, G. D. *Nano Lett.* **2002**, *2*, 583−587.
(29) Cha, J. N.; Shimizu, K.; Zhou, Y.; Christiansen, S. C.; Chmelka, B. F.; Stucky, G. D.; Morse, D. E. *Proc. Natl. Acad. Sci. U.S.A.* **1999**, *96*, 361−365.
(30) Noll, F.; Sumper, M.; Hampp, N. *Nano Lett.* **2002**, *2*, 91−95.

10.1021/cm0504440 CCC: $30.25
Published on Web 07/19/2005

can form at ambient conditions. It is for these reasons that polypeptides have recently drawn considerable attention for assembling inorganic materials.[20−28,31−36] On a different but related theme, recent work in our lab has demonstrated the ability to use polypeptides in different conformations as templates for fabricating porous oxides wherein the size and shape of the pores are determined by the secondary structure of the polypeptide.[37,38] These results have heightened our interest in using biological macromolecules to direct the assembly of complex inorganic materials given that polypeptides have chemical functionality on the molecular level and possess structure on length scales ranging from 1 to 100 nm that can be manipulated and controlled independently.[15,16] In the current work, we turn to a different aspect of polypeptides, namely, that block copolypeptides wherein the blocks have differing solubility will have a propensity to self-assemble into supramolecular equilibrium structures such as micelles and vesicles.

This report is not the first in this area. Cha and co-workers first demonstrated that synthetic cysteine-lysine block copolypeptides can direct the assembly of silica particles with controllable morphologies.[39] Hard silica spheres and well-defined columns of amorphous silica were synthesized by controlling the presence or absence of disulfide linkages. The same copolypeptides were also used to assemble silica and metal nanoparticles[28] (or CdSe/CdS quantum dots[40]) into micron-sized silica hollow spheres. Euliss and co-workers also demonstrated the formation of (EG_2-lysine)-aspartic acid block copolypeptide−nanoparticle composite structure with uniform clusters comprising approximately 20 magnetic nanoparticles.[36] These synthetic peptides open up a new way to synthesize and control materials with structure and function over multiple length scales.

Here, we report the synthesis of spherical nanoparticles in the size range of 20−250 nm using such a biomimetic approach. The synthesis of metal oxide, metal halide, and composite nanospheres is reported. The unique aspect of this investigation compared to previous work is the ability to translate the information content of an individual supramolecular structure into an individual inorganic nanoparticle. The work reported here is proof of concept of translating supramolecular structure of biomimetic soft matter into inorganic hard matter and shows the potential generality of the approach by demonstrating its use in synthesizing a variety of hard matter.

Experimental Section

Block Copolypeptide Synthesis. The amino acids used in this work N_ϵ-Z-L-lysine (∼99%, Fluka, Z: carboxybenzyl) and L-phenylalanine (99%, Aldrich)) were used as received from Aldrich. THF (ACS reagent, Aldrich) and diethyl ether (anhydrous, ACS reagent, VWR) were dried using Na metal. Hexane (ACS reagent, EM Science) was dried using calcium hydride. DMF (ACS reagent, Aldrich) was dried using calcium hydride and was degassed using a freeze−pump−thaw procedure. Triphosgene (98%, Aldrich) was used as received, as was 2,2′-bipyridyl (99+%, Aldrich) and bis-(1,5-cyclooctadiene) nickel (0) (98+%, Strem). 1.0 M HCl in diethyl ether and 33 wt % HBr in acetic acid were used as received from Aldrich. The monomer synthesis and polymer synthesis were performed on a Schlenk line using standard procedures. The nickel initiator 2,2′-bipyridyl-Ni(1,5-cyclooctadiene) (BpyNiCOD) was prepared in a glovebox by ligand exchange of the Ni-bis(COD) complex in the presence of 2,2′-bipyridyl in ether using the procedure described by Binger and co-workers.[41] The N_ϵ-Z-L-lysine (Z-Lys) and L-phenylalanine (Phe) NCAs were synthesized in dry THF using triphosgene as described by Daly and Poche.[42] Diblock copolypeptides were synthesized using N_ϵ-Z-protected L-lysine and L-phenylalanine *N*-carboxyanhydrides (NCAs) using a procedure developed by Deming.[43−45] As reported by Deming, the ring-opening polymerization of the NCAs in the presence of 2,2′-bipyridyl-Ni(1,5-cyclooctadiene) (BpyNiCOD) in dry DMF affords a true living polymerization yielding block copolypeptides of controlled molecular weight and low polydispersity (<1.3). Upon completion of polymerization, the polymer was liberated from the initiator using dilute HCl (1 mM) in diethyl ether and was collected using filtration. The polypeptide was then dissolved in trifluoroacetic acid (99%, Aldrich), and the lysine Z-groups were removed by adding 33 wt % HBr in acetic acid. The polypeptide was then dialyzed and lyophized. ^{1}H NMR of the protected polymer in *d*-TFA was used to verify the composition of the polymer, and gel permeation chromatography was used to determine the molecular weight and polydispersity (Styragel HR4 column, effluent: 10 mM LiBr in DMF, standard: PEO). The Supporting Information contains the GPC data (Table S1, Supporting Information) and the ^{1}H NMR spectra (Figure S1, Supporting Information) of selected polypeptides used in this work. The notation used throughout for the block copolypeptides is Lys_n-*b*-Phe_m, where m and n are the number of amino acids in the respective blocks. Unless noted otherwise, all polymers contain only the L-enantiomer of the amino acids. A few selected polypeptides were synthesized with L-lysine, and a racemic mixture of phenylalanine and these are explicitly labeled as Lys_n-*b*-(rac-Phe)$_m$.

Preparation of Silica Spheres and Hollow Spheres. Silica nanospheres were formed by combining silicic acid with a block copolypeptide solution buffered to pH = 7 with phosphate buffer (J. T. Baker). Orthosilicic acid solution (1 M) was freshly prepared by dissolving tetramethyl orthosilicate (99%, Fluka) in 1 mM HCl to a final concentration of 1 M. As an example, a 2-mL solution of Lys_{23}-*b*-Phe_{23} (0.2 mg/mL) was prepared, and the solution was adjusted to pH = 7 by addition of 0.5 mL phosphate buffer solution. Then, 0.3 mL of freshly prepared orthosilicic acid solution was added to the solution. The solution turned turbid within seconds. The synthesis of silica hollow spheres was complete within 5 minutes. The silica nanospheres were collected by centrifugation at 5000 rpm for 15 min using a Megafuge 2.0 centrifuge (Heraeus Instruments) and were redispersed in DI water by 1 h of sonication.

(31) Zaremba, C. M.; Stucky, G. D. *Curr. Opin. Solid State Mater. Sci.* **1996**, *1*, 425−429.
(32) Coradin, T.; Livage, J. *Colloids Surf., B* **2001**, *21*, 329−336.
(33) Coradin, T.; Durupthy, O.; Livage, J. *Langmuir* **2002**, *18*, 2331−2336.
(34) Coradin, T.; Lopez, P. J. *ChemBioChem* **2003**, *4*, 251−259.
(35) Estroff, L. A.; Hamilton, A. D. *Chem. Mater.* **2001**, *13*, 3227−3235.
(36) Euliss, L. E.; Grancharov, S. G.; O'Brien, S.; Deming, T. J.; Stucky, G. D.; Murray, C. B.; Held, G. A. *Nano Lett.* **2003**, *3*, 1489−1493.
(37) Hawkins, K. M.; Wang, S. S. S.; Ford, D. M.; Shantz, D. F. *J. Am. Chem. Soc.* **2004**, *126*, 9112−9119.
(38) Jan, J.-S.; Shantz, D. F. *Chem. Commun.* **2005**, 2137−2139.
(39) Cha, J. N.; Stucky, G. D.; Morse, D. E.; Deming, T. J. *Nature* **2000**, *403*, 289−292.
(40) Cha, J. N.; Bartl, M. H.; Wong, M. S.; Popitsch, A.; Deming, T. J.; Stucky, G. D. *Nano Lett.* **2003**, *3*, 907−911.
(41) Binger, P.; Doyle, M. J.; McMeeking, J.; Krueger, C.; Tsay, Y.-H. *J. Organomet. Chem.* **1977**, *135*, 405−414.
(42) Daly, W. H.; Poché, D. *Tetrahedron Lett.* **1988**, *29*, 5859−5862.
(43) Deming, T. J. *Nature* **1997**, *390*, 386-389.
(44) Deming, T. J. *J. Am. Chem. Soc.* **1998**, *120*, 4240−4241.
(45) Deming, T. J.; Curtin, S. A. *J. Am. Chem. Soc.* **2000**, *122*, 5710−5717.

The procedure was repeated two times to remove free orthosilicic acid and phosphate. The same experiment shown above was also performed using Tris-HCl buffer (pH 7) instead of phosphate buffer.

Preparation of Silver Bromide (AgBr) Spheres. Silver bromide nanospheres were formed by the addition of aqueous silver nitrate to a solution of block copolypeptide. As an example, a 2-mL solution of Lys_{23}-*b*-Phe_{23} (0.2 mg/mL) in DI water was prepared, and 1 mL of 0.171 N silver nitrate solution was added to it. Aliquots of silver nitrate solution were added until the particle size measured by dynamic light-scattering did not change. Then, the solution was incubated at ambient temperature for several hours and the color of the solution changed from yellow to brown. The AgBr spheres were collected by centrifugation at 6000 rpm for 30 min using a Megafuge 2.0 centrifuge (Heraeus Instruments).

Preparation of AgBr/Silica Core−Shell Nanospheres. AgBr/silica core−shell nanospheres were prepared as follows. A 2-mL solution of Lys_{80}-*b*-$(rac\text{-}Phe)_{10}$ (1.2 mg/mL) in DI water was prepared and to it 0.8 mL of 0.00171 N silver nitrate solution was added. After 30 min of incubation, the solution was adjusted to pH = 7 by adding 0.8 mL of pH = 7 phosphate buffer solution. Then, 0.4 mL of freshly prepared orthosilicic acid solution was added. The mixture rapidly turned turbid, and within 5 minutes the formation of AgBr/silica core−shell nanospheres was complete. The AgBr/silica core−shell nanospheres were collected by centrifugation at 5000 rpm for 15 min using a Megafuge 2.0 centrifuge (Heraeus Instruments) and were redispersed in DI water by 1 h of sonication. The procedure was repeated two times to remove free orthosilicic acid, phosphate, and silver ions.

Preparation of AgBr−Rhodamine 6G Rods. Two tenths of a milliliter of silver nitrate solution (0.171 N) was added to a 2-mL Lys_{80}-*b*-$(rac\text{-}Phe)_{10}$ solution (2 mg/mL). After 30 min of incubation, 0.6 mL of rhodamine 6G solution (5.5 mM) was added to the solution, and AgBr-Lys_{80}-*b*-$(rac\text{-}Phe)_{10}$-rhodamine 6G rods formed. Dilution of this suspension with 18 mL DI water leads to recovery of the silver bromide nanospheres.

Analytical. Gel permeation chromatography measurements were performed before deprotection of the polypeptides using a Shimadzu system consisting of one Styragel HR4 (Waters) column, eluted with 10 mM LiBr in DMF at 25 °C. The eluent flow rate was 1 mL/min. Calibration was performed using poly(ethylene oxide) standards. ^1H NMR spectra were recorded at 300 MHz on a Mercury 300 Varian spectrometer using *d*-TFA as solvent. Critical aggregation concentrations (cac) were determined by measuring the conductivity of block copolypeptide solutions as a function of polypeptide concentration (0.001−1 mg/mL). The conductivity measurements were performed with an Accumet AB30 conductivity meter with a conductivity cell (0.1 cm^{-1} cell constant). Dynamic light-scattering measurements were carried out using a Brookhaven ZetaPALS instrument. Vertical polarized light with a wavelength of 658 nm was used as the incident beam. The intensity of the scattered light was measured at a 90° scattering angle unless specified and was temperature controlled at 25 °C. Time-averaged particle size distributions were collected over an analysis time of at least 10 min. Dynamic light-scattering measurements at different scattering angles (30°, 45°, 60°, 90°, 120°, 135°, and 150°) were performed with a Brookhaven Instruments BI-200SM goniometer using a Melles Griot HeNe laser with a wavelength of 633 nm. The hydrodynamic diameter (D_h) of the polypeptide supramolecular structures was determined from light-scattering experiments using Brookhaven Instruments Dynamic light-scattering software. For the measurement of vesicles formed by block copolypeptides dissolved in DI water, the samples were prepared and were followed by centrifugation at 6000 rpm for 30 min using a Megafuge 2.0 centrifuge (Heraeus Instruments). The upper portion of each solution was transferred into a rectangular light-scattering cell. The AgBr suspensions were measured directly without any treatment. The silica and AgBr/silica core−shell nanosphere suspensions were immediately diluted to $^1/_{10}$ of their original concentration, and then a small amount of nonionic surfactant (Igepal CO-720) was added to the suspensions. The suspensions were measured after 1 h of sonication. Field-emission scanning electron microscopy (FE-SEM) measurements were performed using a Zeiss Leo-1530 microscope operating at 1−10 kV. The microscope employs a GEMINI electron optical column with a Schottky-type field emitter, single condenser, crossover-free beam path, large specimen chamber with two chamber ports for EDS or WDS adaptation, four accessory ports on the chamber and three on the door, fail-safe vacuum system, and digital image store and processor. Samples were collected via centrifugation, were air-dried, and were mounted on carbon tape for imaging. Transmission electron microscopy (TEM) measurements were performed on a JEOL 2010 microscope with a LaB_6 filament and an excitation voltage of 200 kV. The samples were dispersed in methanol (100%, Aldrich) and were placed on a 400-mesh copper grid. Energy-dispersive X-ray analysis (EDX) was performed using an Oxford instrument eXL EDS system. Powder X-ray diffraction (PXRD) measurements were performed on a Bruker GADDS three-circle X-ray diffractometer (Cu Kα radiation) in reflection mode from $2\theta = 5$ to 70° with a step size of 0.03° and 2 s per step. Infrared spectroscopy was performed on a Thermo Nicolet Nexus 670 FTIR. Background spectra were collected after 30 min of evacuation. A powder mixture of mass ratio 0.01 sample: 0.99 potassium bromide (Aldrich) was pelletized and analyzed after 30 min of evacuation. Sixty-four scans were acquired per spectrum. Confocal images were captured with Carl Zeiss LSM 5 PASCAL inverted confocal microscope equipped with a 63× oil immersion objective (NA = 1.4). The laser excitation wavelength was 632 nm. Samples were mounted on glass slides.

Table 1. Hydrodynamic Diameter of the Vesicles Formed by the Lys-Phe Diblock Copolypeptides and the Contour Lengths of Individual Chains

copolypeptide	$<D_h>$ (nm)	contour length (nm)
Lys_{12}-*b*-Phe_4	107 ± 6	∼6
Lys_{24}-*b*-$(rac\text{-}Phe)_4$	121 ± 5	∼9
Lys_{23}-*b*-Phe_{23}	125 ± 2	∼15
Lys_{32}-*b*-Phe_5	183 ± 8	∼12
Lys_{80}-*b*-$(rac\text{-}Phe)_{10}$	226 ± 10	∼28
Lys_{150}-*b*-Phe_{15}	413 ± 20	∼51

Results and Discussion

Block Copolypeptide Solution Behavior. The diblock copolypeptides synthesized have a mismatch in solubility between the lysine block (highly water soluble at pH = 7) and the phenylalanine block (poorly water soluble) that leads to their aggregation in solution. The nature of the structures formed in solution by the diblock copolypeptides was probed using dynamic light-scattering (DLS). DLS measurements performed at several scattering angles (30°, 45°, 60°, 90°, 120°, 135°, and 150°) indicate that the objects in solution are spherical, and the hydrodynamic diameters determined at the different angles are all within 3% of one another. Table 1 summarizes the hydrodynamic diameters and contour lengths of the structures formed. As can be seen in Figure 1, the objects present in solution are an order of magnitude larger than the contour lengths of the chains. The contour lengths calculated for the polypeptide chains[28] and the size of the scatterers in solution on the basis of DLS are consistent with the formation of vesicles. Static light-scattering mea-

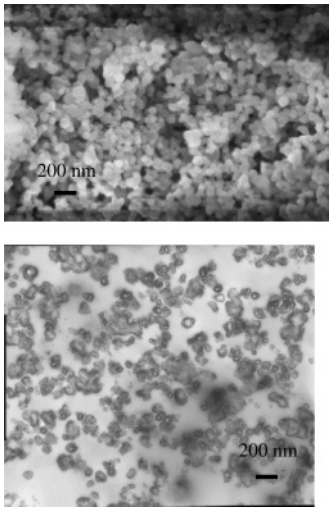

Figure 1. FE-SEM (top) and TEM (bottom) images of hollow silica spheres synthesized using Lys_{23}-*b*-Phe_{23} as template.

surements are also consistent with the presence of vesicles (Supporting Information). From Table 1, the copolypeptides with higher molecular weight and Lys/Phe block ratios form larger vesicles. For a fixed block ratio of approximately 7 Lys:1 Phe (e.g., Lys_{80}-*b*-(rac-Phe)$_{10}$, Lys_{32}-*b*-Phe_5, and Lys_{24}-*b*-(rac-Phe)$_4$), increasing the molecular weight leads to larger vesicles. For an approximately fixed molecular weight, increasing the Lys:Phe ratio also leads to larger vesicles. This latter point is likely due to the lysine block adopting an extended conformation at pH = 7 to minimize unfavorable side chain electrostatic repulsive forces given that this is well below the pK_a of the N_ϵ-amine group (9.5−10).[46] DLS measurements were performed on Lys-*b*-Phe copolypeptides with varying electrolyte content to verify if screening the electrostatic repulsion of the side chain groups would modify the vesicle size. Those experiments show that the vesicle size decreases with increasing electrolyte concentration. When the (NaBr) concentration is 0.4 M, the vesicles are approximately 80% of their original size. A more comprehensive study of the solution behavior of these macromolecules is forthcoming, but the results above clearly demonstrate that the Lys-*b*-Phe copolypeptides adopt well-defined supramolecular structures (in this case vesicles) in solution.

Formation of Silica Spheres and Hollow Spheres. Having demonstrated that the block copolypeptides assemble into well-defined structures, studies were then performed to determine if the structures could be used as templates for inorganic material growth. Using vesicles formed from Lys_{23}-*b*-Phe_{23} as a template, it is possible to synthesize hollow silica nanospheres at pH = 7 using orthosilicic acid as the silica source (Figure 1). DLS measurements show that the hydrodynamic diameter of the nanospheres is 114 nm, consistent with the FE-SEM images obtained. TEM images of the same sample show that the spheres are hollow (Figure 1). In contrast, silicas synthesized using poly-L-lysine·HBr under comparable conditions possess a platelike morphology (see Table S1, Figure S2 Supporting Information). The observance

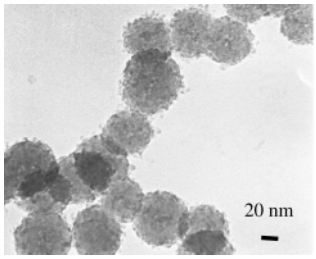

Figure 2. TEM image of silica spheres synthesized using Lys_{80}-*b*-(rac-Phe)$_{10}$ as template.

of platelike morphologies for the pure homopolymers is consistent with recent work published by Rodriguez and coworkers[47] of the biosilicification of poly-L-lysine with different molecular weight under chemical influences.

The block ratio of the Lys:Phe copolypeptide strongly influences the structure of the materials obtained. It is observed that when the block ratio of Lys:Phe is increased above 1:1, the silica spheres formed are not hollow and are smaller than the corresponding copolypeptide vesicle. Figure 2 shows the TEM image of silica spheres made using Lys_{80}-*b*-(rac-Phe)$_{10}$ (1 mg/mL) as the template, and as can be seen, the spheres are not hollow. The critical aggregation concentration (cac) of Lys_{80}-*b*-(rac-Phe)$_{10}$ is 0.03 mg/mL, so the concentration of Lys_{80}-*b*-(rac-Phe)$_{10}$ in the synthesis is well above the cac. Consistent with the solution behavior, increasing the molecular weight for an approximately constant Lys:Phe block ratio (e.g., Lys_{80}-*b*-(rac-Phe)$_{10}$, Lys_{32}-*b*-Phe_5, and Lys_{24}-*b*-(rac-Phe)$_4$) leads to larger silica nanospheres. In contrast to the solution behavior, increasing the Lys:Phe block ratio for an approximately constant molecular weight leads to smaller nanospheres. Given the highly extended conformation of the poly-L-lysine at pH = 7, it appears that for copolypeptides with larger lysine blocks or higher Lys/Phe block ratios, the vesicles are not stable during silica formation. Additionally, it would seem likely that the lysine blocks become less extended during silica precipitation. To study this, a set of silicas were made using Lys_{80}-*b*-(rac-Phe)$_{10}$ as template in the presence of salt (NaBr). The size of spheres made using Lys_{80}-*b*-(rac-Phe)$_{10}$ as template with no NaBr added is between 50 and 90 nm. However, the size of particles made using Lys_{80}-*b*-(rac-Phe)$_{10}$ as template in the presence of 1 M NaBr is 30 nm and smaller. This result is qualitatively consistent with increased electrolyte concentration causing a decrease in the effective lysine block length.

The silicas formed are relatively insensitive to the orthosilicic acid concentration over the range of 0.05−1 M. However, the copolypeptide concentration does affect the silicas formed, the most notable difference being particle polydispersity. For example, a broader size distribution (50−400 nm) of silica particles was synthesized using Lys_{80}-*b*-(rac-Phe)$_{10}$ (6 mg/mL) as template (Figure S3, Supporting Information) as compared to those made with a lower polypeptide concentration. IR spectra of all as-made silica materials clearly show the presence of the amide I and II

(46) Barret, G. C. *Amino Acids and Peptides*; Cambridge University Press: Cambridge, U.K., 1998.

(47) Rodríguez, F.; Glawe, D. D.; Naik, R. R.; Hallinan, K. P.; Stone, M. O. *Biomacromolecules* **2004**, *5*, 261−265.

Table 2. Vesicle Hydrodynamic Diameter and AgBr Sphere Hydrodynamic Diameter as Measured by DLS

copolypeptide	$<D_h>$ of vesicles (nm)	$<D_h>$ of AgBr spheres (nm)
Lys_{12}-*b*-Phe_4	107 ± 6	145 ± 5
Lys_{23}-*b*-Phe_{23}	125 ± 2	125 ± 3
Lys_{12}-*b*-$(rac\text{-}Phe)_{10}$	226 ± 10	250 ± 10

bands, indicating that the copolypeptides are incorporated in the material.

As a comparison to existing literature, Kröger and coworkers[21] used silaffin-1A extracted from diatom to precipitate silica nanoparticles 500−700 nm in size. In that paper, they claimed that phosphate is required for the precipitation of silica. To study this in more detail here, the effect of phosphate ions was probed by performing syntheses using the block copolypeptides above with Tris-HCl buffer in lieu of phosphate buffer. It is observed that the copolypeptides still can precipitate silica using Tris-HCl buffer (pH 7) instead of phosphate buffer. However, smaller silica particles (less than 20 nm) were formed than those made in the presence of phosphate buffer (Figure S4, Supporting Information).

Formation of AgBr Nanospheres. Another approach to translating the size of the vesicles into an inorganic phase is to use the reaction between silver ions and bromide ions,[48−50] given the low solubility of silver halides in water and that the lysine blocks have bromide counterions. Table 2 shows the hydrodynamic diameter of vesicles and templated AgBr spheres. Dynamic light-scattering (DLS) analysis shows that the vesicle size is comparable to the AgBr spheres. FE-SEM images (Figure 3) are consistent with DLS measurements. AgBr spheres of controllable size were synthesized using diblock copolypeptides as templates. The size of the AgBr particles can be adjusted on the basis of the copolypeptide used and the amount of $AgNO_3$ added to the block copolypeptide solution. As an example of this, AgBr spheres between 20 and 250 nm can be synthesized using Lys_{80}-*b*-$(rac\text{-}Phe)_{10}$ as template by controlling the amount of silver nitrate added. Silver bromide spheres as small as 20 nm can be synthesized as shown in Table 3 and Figure 4. This result shows the possibility of controlling the AgBr sphere size on the basis of the amount of silver nitrate added to solutions of block copolypeptides. The as-made AgBr nanospheres were not hollow because AgBr coalesced during the synthesis. This is proved by dynamic light-scattering measurements as the AgBr particle size is observed to increase with incremental addition of silver nitrate. The maximum particle size obtained in all cases corresponds to the vesicle diameter. Powder X-ray diffraction (not shown) shows that all materials formed are AgBr.

Formation of AgBr/Silica Core−Shell Spheres. A logical extension of the work above is the synthesis of core−shell nanospheres using block copolypeptides. All copolypeptides can be used to synthesize AgBr/silica core−shell spheres. Figure 4 shows the TEM images of AgBr/silica core−shell spheres using Lys_{80}-*b*-$(rac\text{-}Phe)_{10}$ as template.

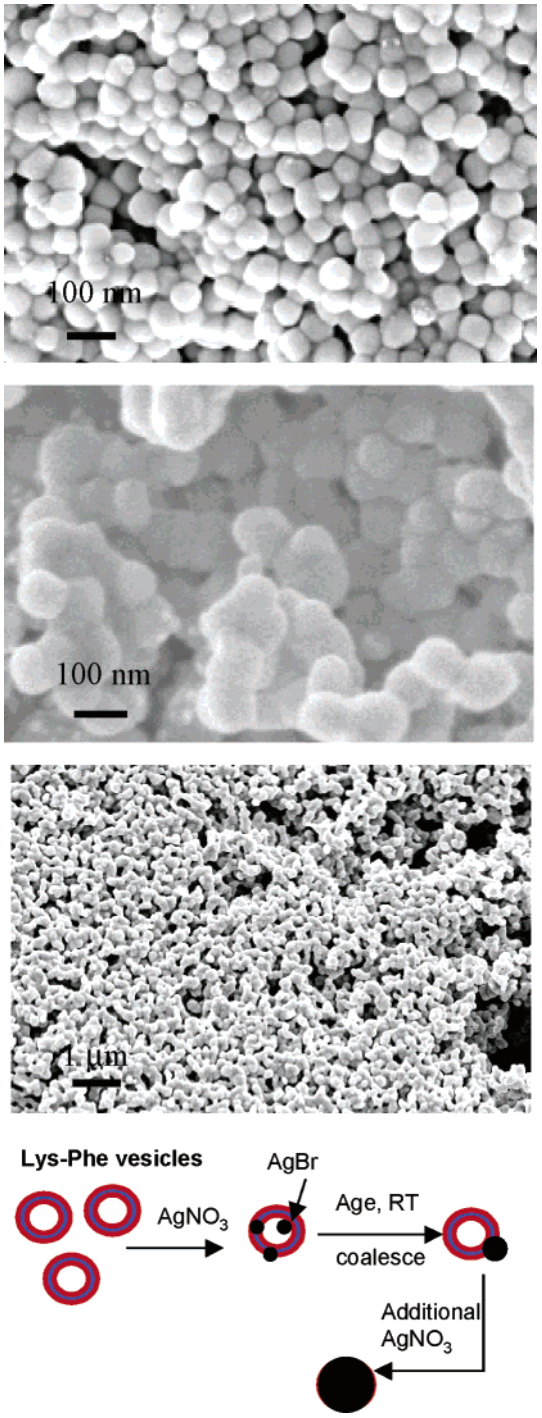

Figure 3. FE-SEM image of AgBr spheres synthesized using (from top to bottom) Lys_{12}-*b*-Phe_4, Lys_{23}-*b*-Phe_{23}, and Lys_{80}-*b*-$(rac\text{-}Phe)_{10}$ as template. (bottom) Proposed mechanism of particle growth.

Table 3 (entries a and c) shows that the size of the silver bromide core can be adjusted on the basis of the amount of silver nitrate added to the solution, consistent with the results above. The size of the core−shell spheres is smaller than the size of the Lys_{80}-*b*-$(rac\text{-}Phe)_{10}$ vesicles. This is because the addition of orthosilicic acid causes the lysine block to collapse. Some spheres have more than one AgBr particle in their core. This is because either (1) multiple AgBr particles nucleate in some of the vesicles or (2) the spheres fuse together during the precipitation of silica. On the basis of the TEM and SEM results, we believe it is the first point as large silica aggregates are not observed. The size of the

(48) Xu, S.; Li, Y. D. *J. Mater. Chem.* **2003**, *13*, 163−165.
(49) Gong, H.; Liu, M. *Chem. Mater.* **2002**, *14*, 4933−4938.
(50) Ohde, H.; Rodriguez, J. M.; Ye, X.-R.; Wai, C. M. *Chem. Commun.* **2000**, 2353−2354.

Table 3. Hydrodynamic Diameter of AgBr and AgBr/Silica Core−Shell Nanospheres Measured by DLS[a]

sample	synthesis condition	$<D_h>$ of AgBr (nm)	$<D_h>$ of AgBr/silica (nm)
a	2 mL of Lys_{80}-*b*-(rac-$Phe)_{10}$ (1.2 mg/mL), 0.8 mL of $AgNO_3$ (0.0017 N)	22 ± 2	202 ± 10
b	2 mL of Lys_{80}-*b*-(rac-$Phe)_{10}$ (1 mg/mL), 1.2 mL of $AgNO_3$ (0.0017 N)	28 ± 3	158 ± 8
c	2 mL of Lys_{80}-*b*-(rac-$Phe)_{10}$ (1 mg/mL), 2 mL of $AgNO_3$ (0.0017 N)	40 ± 3	112 ± 6

[a] The DLS data of AgBr/silica core−shell nanospheres showed some aggregates resulting in the higher D_h values.

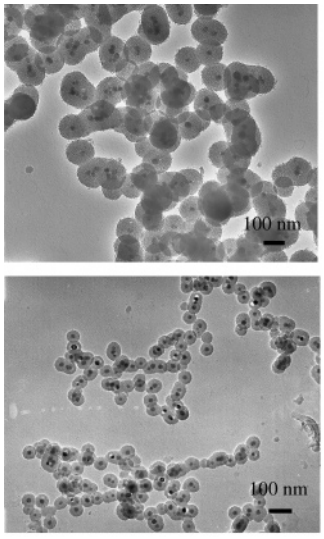

Figure 4. TEM images of AgBr/silica core−shell spheres, sample a (top) and c (bottom) in Table 3.

AgBr core and the thickness of silica shell can be independently varied by changing the amount of silver nitrate and using different copolypeptides. The contrast difference between the core and the shell observed in the TEM images is attributed to the different compositions on the two parts. Before silica was coated on the shell, DLS measurements were performed on the AgBr particles and the particle size was consistent with the TEM images. After coating silica on the shell, DLS measurements were again performed on the core−shell spheres. The synthesis conditions and characterization data of AgBr and AgBr/silica core−shell spheres measured by DLS are summarized in Table 3. The particle size measured by DLS is slightly higher than the size estimated by TEM; this is likely due to some of the particles aggregating. Powder X-ray diffraction data indicates the presence of crystalline silver bromide. Again, IR spectra of all samples show the presence of the amide I and II bands, indicating that copolypeptides are incorporated in the material. These results show that it is possible to manipulate the size of the AgBr core and silica shell independently on the basis of the synthesis conditions.

Hollow silica spheres can also be made by simply calcining the AgBr/silica core−shell spheres (sample b) at 550 °C (6 h). Figure 5 shows FE-SEM and TEM images of hollow silica spheres (sample b in Table 3) and EDX analysis on the silica shell. It clearly shows that the spheres are hollow and intact after calcination. EDX analysis on the shell of the hollow spheres shows the presence of silver but no trace of bromine, indicating that AgBr melts (melting point 432 °C for bulk material), leaving the core through the pores during calcinations. On the basis of the EDX results, silver is still present in these materials, though large silver particles are not detected by TEM/PXRD. However, some of the

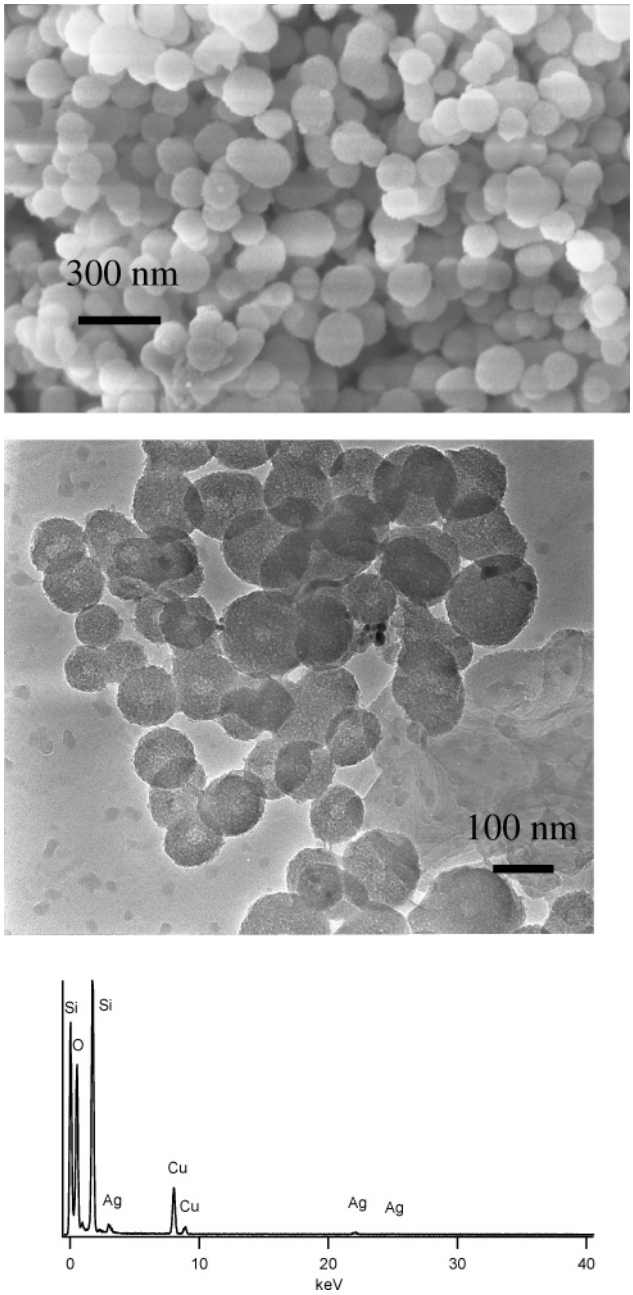

Figure 5. FE-SEM and TEM images of hollow silica spheres (sample b in Table 3) and EDX analysis on the silica shell.

spheres (sample a in Table 3) still contain silver in the core as can be seen in the TEM images. EDX analysis confirms the presence of silver in the core. From these analyses, it is not clear whether the silver is present as metallic silver or silver oxide, however, the latter seems more likely.

Attempts were also made to synthesize Ag/silica core−shell particles. The synthesis procedure is the same as that used to prepare AgBr/silica core−shell spheres (sample a in Table 3), except that $NaBH_4$ solution is added to perform the reduction after the formation of AgBr nanoparticles. A

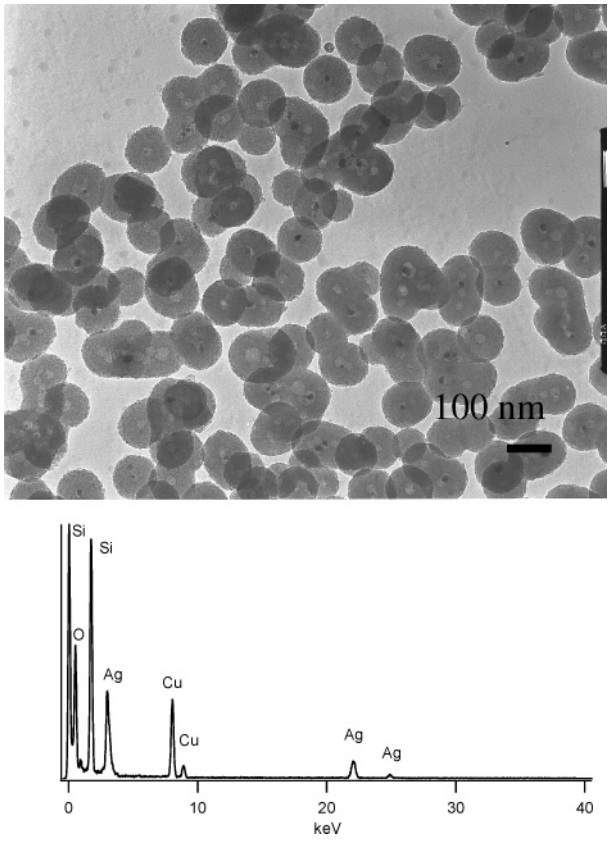

Figure 6. TEM image of hollow silica spheres (sample a in Table 3) and EDX analysis on the particle in the core.

similar preparation of silver nanoparticles from insoluble salts (AgCl or AgBr) has been reported in the literature.[51] From the TEM image and EDX analysis on the core (Figure S5, Supporting Information), core−shell spheres using $Lys_{80}(rac\text{-}Phe)_{10}$ as template can be synthesized. EDX of the core shows the presence of silver and no trace of bromine. The oxidation state of the silver is not known although the EDX rules out the presence of AgBr. DLS and TEM, however, indicate that the core−shell particles formed using this approach are not as homogeneous as the AgBr/silica particles formed. Current work is exploring this and the oxidation state of the silver in these materials.

Formation of AgBr−Rhodamine 6G Rods. Figure 7 shows the confocal, FE-SEM, and TEM images of AgBr−rhodamine 6G rods formed by the addition of rhodamine 6G to a suspension of silver bromide nanoparticles. The rods are square (1 μm × 1 μm) and 10 μm in length. The TEM image shows that the rod surface is comprised of AgBr nanoparticles. Dye metal halide composites have been extensively used in color photography.[52,53] The dye molecules closely pack on the particle surface leading to aggregation,[54,55] which is also observed in heterogeneous media such as micelles[56,57] and vesicles.[58] The critical concentration of rhodamine 6G needed to form the rods is approximately 5.5 mM. In a control experiment, irregular aggregates were formed by adding rhodamine 6G solution (5.5 mM) to a silver nitrate solution (0.107 N) (Figure S6, Supporting Information). These aggregates are rhodamine 6G/AgCl particles that form because of the presence of chloride ions. From the results of the control experiment, the Lys_{80}-*b*-$(rac\text{-}Phe)_{10}$/AgBr nanoparticle hybrids lead to well-dispersed rods, whereas molecular silver precursors do not. Perhaps more significant is that the rods reversibly disassemble simply by diluting the solution to $^1/_{10}$ of the original concentration. The EDX results in Figure 8 show that the interior of the rods is organic material, and the surface of the rods contains silver, bromine, and chlorine.

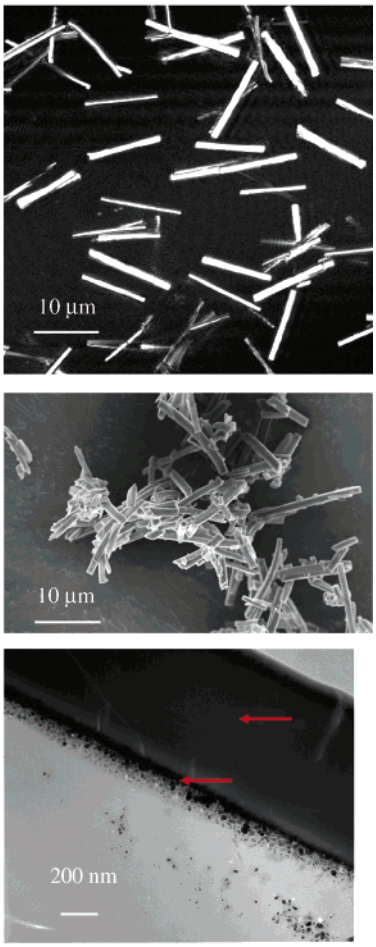

Figure 7. Confocal microscopy (top), FE-SEM (middle), and TEM (bottom) images of AgBr rods assembled from AgBr/block copolypeptide hybrid particles. The arrows show the locations for the EDX analysis shown in Figure 8.

Conclusions

This paper outlines a general approach to the synthesis of inorganic nanoparticles of controllable size on the basis of

(51) Yonezawa, T.; Genda, H.; Koumoto, K. *Chem. Lett.* **2003**, *32*, 194−195.
(52) James, T. H. *Theory of Photographic Processes*; Macmillan Publishing Co.: New York, 1977.
(53) Chanon, M. *Homogeneous Photocatalysis;* John Wiley & Sons Ltd: New York, 1997.
(54) Nasr, C.; Liu, D.; Hotchandani, S.; Kamat, P. V. *J. Phys. Chem.* **1996**, *100*, 11054−11061.
(55) Sayama, K.; Sugino, M.; Sugihara, H.; Abe, Y.; Arakawa, H. *Chem. Lett.* **1998**, 753−754.
(56) Kelkar, V. K.; Valalulikar, B. S.; Kunjappu, J. T.; Manohar, C. *Photochem. Photobiol.* **1990**, *52*, 717−721.
(57) Mialocq, J. C.; Hebert, P.; Armand, X.; Bonneau, R.; Morand, J. P. *J. Photochem. Photobiol.* **1991**, *56*, 323−338.
(58) Deumie, M. D.; Lorente, P.; Morizon, D. *Photochem. Photobiol.* **1995**, *89*, 239−245.

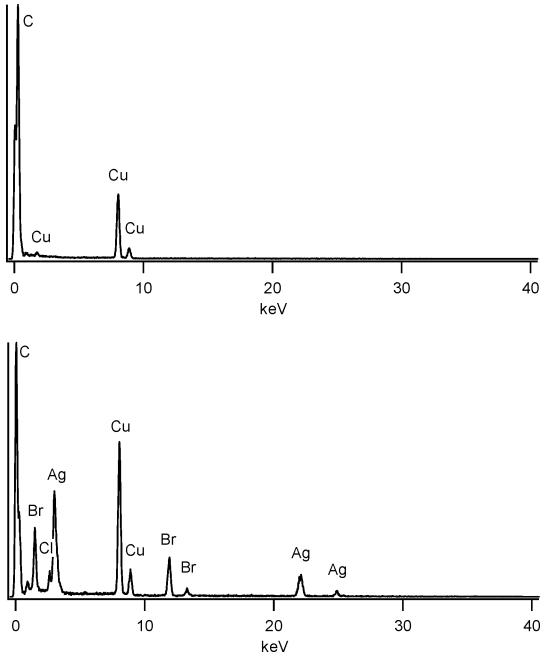

Figure 8. EDX analysis on the interior (top) and edge (bottom) of the rods shown in Figure 7.

the use of block copolypeptides as templates. The synthesis of silica, AgBr, and AgBr/silica core−shell nanospheres with controllable particle size and structure is investigated. Under a narrow range of polypeptide compositions, hollow silica spheres with controllable cavity size and shell thickness can be designed and synthesized. Using the same methodology, other metal halides and ordered structures can be synthesized by using different block copolypeptides and metal sources. The ease with which these well-defined and controllable inorganic structures can be made opens up the possibility to design multicomponent materials with spatially defined arrangements of the different components and using them for applications such as semiconductor, molecular sieving, and chemical storage. The organic template itself may have interesting applications as well, such as drug delivery. To this end, the phase behavior and self-assembly of these block copolypeptides as well as other templated inorganic materials are under continued investigation.

Acknowledgment. D. F. S. acknowledges financial support from Texas A&M University and the Texas A&M University Life Science Task force. The authors gratefully acknowledge Prof. Dave Bergbreiter (Chemistry, TAMU) for access to the GPC instrumentation; the Microscopy and Imaging Center at Texas A&M for access to the FE-SEM, TEM, and EDX instrumentation; and the Chemistry Department at Texas A&M for access to the NMR and X-ray diffraction facilities. The FE-SEM acquisition was supported by the National Science Foundation under Grant No. DBI-0116835.

Supporting Information Available: Characterization of block copolypeptides using ^{1}H NMR and GPC. Analysis of static light-scattering data for the block copolypeptide solutions. FE-SEM image of silica plates synthesized using poly-L-lysine·HBr as template. FE-SEM and TEM images of silica spheres synthesized using Lys_{80}-*b*-$(rac\text{-}Phe)_{10}$ as template. FE-SEM image of silica synthesized using Lys_{80}-*b*-$(rac\text{-}Phe)_{10}$ (2 mg/mL) as template and 50 mM Tris-HCl buffer (pH 7). TEM image of Ag/silica core−shell spheres and EDX analysis on the core. Confocal microscopy image of rhodamine 6G/AgCl aggregates (word/PDF). This material is available free of charge via the Internet at http://pubs.acs.org.

CM0504440